EFFECT OF THERMOMECHAINCAL PROCESSING ON FATIGUE CRACK PROPAGATION IN INCONEL ALLOY 783

L. Z. Ma*, K. M. Chang*, S. K. Mannan**, S. J. Patel**
* West Virginia University, Morgantown, WV
** Special Metals Corporation. Huntington, WV

Abstract

Recently developed INCONEL® alloy 783 (nominal composition of Ni-34Co-26Fe-5.4Al-3Nb-3Cr) is precipitation strengthened by Ni_3Al-type γ' and NiAl-type β phases. Due to its low coefficient of thermal expansion, high strength, and good oxidation resistance, alloy 783 is used for casings and bolting applications in gas turbines. During thermomechanical processing (TMP), the high Al content in alloy 783 results in the formation of β phase in an austenite matrix. The size and distribution of β phase governs the microstructure of the alloy. Therefore, optimization of TMP is critical for microstructure and mechanical properties. This study presents the effect of TMP on fatigue crack growth in alloy 783, especially in time-dependent condition.

Initially, the material was hot rolled in the mill at 1095°C. This was followed by rolling in the laboratory to 50% reduction at temperatures of 870°C, 1010°C and 1150°C. Materials rolled in the mill and laboratory were direct aged without solution annealing. The aged materials were subjected to fatigue crack growth testing at room temperature, 300 °C, 450 °C and 600 °C and constant stress intensity mode. The results exhibit that time-dependent fatigue crack propagation resistance of alloy 783 can be dramatically improved by TMP. Comprehensive microstructure characterization and fractographic analysis suggests that the enhancement of fatigue crack growth in time-dependent condition is associated with the change of fracture mode. The SAGBO (Stress Accelerated Grain Boundary Oxidation) mechanism and damage zone model were applied to explain these phenomena.

Introduction

Over the past twenty years, high strength low coefficient of thermal expansion (low CTE) superalloys, such as INCOLOY® alloy 903, 907, and 909, have been used for compressor cases, rings and shrouds to enable higher efficiency of gas turbine engines through tighter control of blade tip clearances over the range of turbine operating conditions [1-3]. The ferromagnetic characteristic below the Curie points of these alloys is responsible for thermal expansion coefficients lower than observed in paramagnetic alloys. These Ni-Fe-Co base alloys also have very low chromium content, as added Cr lowers the Curie temperature and thereby increase overall thermal expansion rate [4]. However, low content of Cr makes these alloys susceptible to stress accelerated grain boundary oxidation (SAGBO). INCONEL alloy 783 was developed to have low CTE and superior SAGBO and surface oxidation resistance than comparable alloys [1-3].

Relative to the INCOLOY Alloy 900-series of low CTE superalloys, alloy 783 with Al above 5% employs a three-phase microstructure (γ-γ'-β) to control mechanical properties, SAGBO and oxidation resistance. Fine γ' (Ni_3Al, Nb) precipitates form at low temperature aging treatments and provide adequate alloy strength [5]. The formation of the unique β phase (NiAl) is responsible for the improvement in SAGBO and oxidation resistance. The β phase is made possible by the high Al content in this alloy. Since β particles are heterogeneous and precipitate both in the grain boundaries and intrangranularly in the dislocation networks, thermomechanical processing (TMP) can be utilized to control their precipitation kinetics and thereby control the properties and microstructure of this alloy. Early work has shown that TMP has a significant effect on microstructure and room temperature properties of alloy 783 [6]. The present study investigates how TMP affects fatigue crack propagation in this alloy.

® INCONEL and INCOLOY are trademarks of the Special Metals family of companies.

Material and experimental procedure

The INCONEL alloy 783 used in this study was supplied from regular production material by Special Metals Corporation, Huntington, WV. An ingot of 500mm diameter was vacuum induction melted (VIM) and vacuum arc remelted (VAR) using standard superalloy melting practices. The ingot chemical analyses are given in Table I

Superalloys 2000
Edited by T.M. Pollock, R.D. Kissinger, R.R. Bowman,
K.A. Green, M. McLean, S. Olson, and J.J. Schirra
TMS (The Minerals, Metals & Materials Society), 2000

Table I. Chemical Composition (wt%) of INCONEL Alloy 783

Element	Analyzed Results	Nominal Composition
Ni	28.21	28
Fe	24.88	Bal.
Co	34.39	34
Al	5.32	5.4
Nb	3.11	3.0
Ti	0.32	0.2 max
Cr	3.24	3.0

The precipitation temperature of two major phases in alloy 783, γ' (Ni_3Al) and β (AlNi), is respectively from 600°C to 800°C and from 700°C to 1140°C [1, 2, 6]. Therefore, TMP of this alloy is usually performed in the β precipitation temperature range to employ the β precipitates for structure control. Upon homogenization, the ingot was converted into billet in flat bar form at 1120°C. The received flat bar for this study was rolled to 19mm at 1095°C, which was designated as the primary rolling (HR0). This piece was used as a reference for the other three TMP procedures, which received a final rolling at specified rolling temperatures. Once the rolling temperature was reached, the plate was hot rolled at a 50% reduction ratio to 9.5mm thick. The first TMP rolling (HR1) was set at 870°C, which is above the γ' solvus, but still at the bottom of the β precipitation zone. The second rolling temperature (HR2) was chosen at 1010°C, which falls in the middle of the β precipitation zone. A last section (HR3) was rolled above the β solvus at 1150°C. Table II summarizes all TMP schemes used in the present work.

Specimens were machined from all the plates receiving the different TM schedules in the longitudinal direction, and received a direct aging heat treatment as follows: 843°C/4h, air cool + 720°C/8h, furnace cool at 55°C/hr to 620°C, hold at 620°C for 8 hours then air cool. The direct age, which eliminates the solution annealing, can markedly show the effect of TMP processing.

Table II. TMP Parameters

HR0	Primary roll at 1095°C
HR1	Primary roll + 50% reduction at 870°C
HR2	Primary roll + 50% reduction at 1010°C
HR3	Primary roll + 50% reduction at 1150°C

Fatigue crack propagation (FCP) tests were conducted at room temperature, 300°C, 450°C and 600°C respectively by using single edge-notched tension specimens. Crack length was monitored continuously by a D.C potential drop system. A MTS servohydraulic system equipped with the quartz light heaters heated the specimens to temperature to an error of around ±6°C. This test system can be completely monitored by a computer during the FCP test for either constant stress intensity factor mode or constant load mode. A sinusoidal fatigue cycle of 10 Hz was adopted to examine the crack propagation under pure fatigue. A slower fatigue cycle of 1/3 Hz was used to measure the effect of frequency on FCP. A third fatigue waveform consisting of a 1/3 Hz sinusoidal fatigue cycle and 100 seconds hold time at the maximum load of each cycle was also used, which usually results in time-dependent crack growth for several superalloys during elevated temperature fatigue [7-9].

FCP tests for every TMP specimen were conducted at constant stress intensity factor (ΔK) mode, Kmax = 28 MPa√m. The maximum-minimum load ratio (R) was kept at 0.05 in all waveforms. FCP tests were performed continuously from high temperature to low temperature, and from high frequency to low frequency. All specimens were precracked under fatigue condition of Kmax = 28 MPa√m, R= 0.05, f = 10 Hz and room temperature.

Each specimen was broken into halves when the test was finished. Many beach marks associated with the change of test temperature were observed on the fracture surface as seen in Figure 1. The measurement of beach marks was made for crack-length and ΔK value calibration. The linear regression was employed to calculate crack growth rate based on crack length vs. number of cycle's results.

Metallographic samples were prepared using conventional mechanical grinding and polishing procedures according to standard laboratory practices. Kalling's reagent consisting of 6 gm $CuCl_2$, 100 ml HCl, 100 H_2O, and 100 ml CH_3OH was used to reveal the microstructure. Scanning electron microscopy was used to examine the fracture surfaces of every sample.

Results

Microstructure

Figure 2 illustrates the microstructure of the alloy after TMP and direct aging. As expected, due to the high rolling temperature and no secondary deformation, the sample hot rolled at 1095°C (HR0) shows typically equiaxed recrystallized grains, with a grain size of ASTM 12-13, as seen in Figure 2(a). However, samples hot rolled at 870°C (HR1) and 1010°C (HR2) exhibit hot worked microstructure containing elongated β particles and stringers, as seen in Figure 2 (b) and (c). The sample hot rolled at 1150 °C (HR3) displays a dynamically recrystallized serrated grain boundary microstructure containing intergranular and transgranular β phase particles, as seen in Figure 2(d).

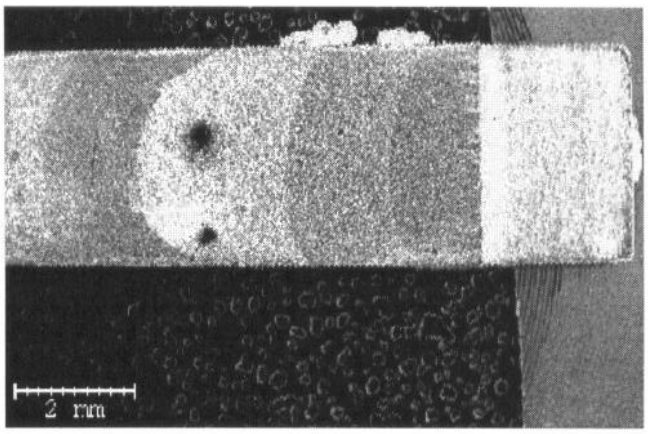

Figure 1: Specimen profile after FCP testing

Fatigue Crack Propagation

Constant ΔK crack propagation curves at 600°C for two hot rolled materials, HR1 and HR3, are presented in Figures 3 (a) and

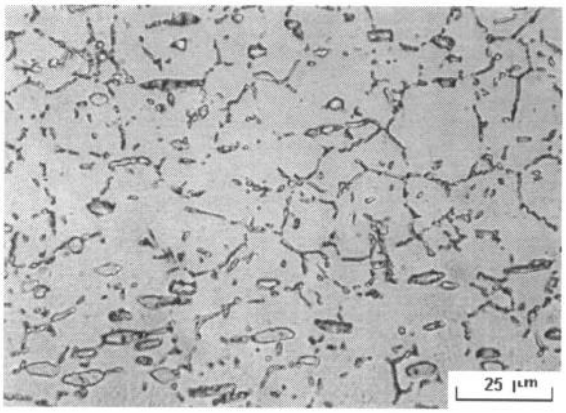

Figure 2 (a): Hot rolling at 1095°C (HR0)

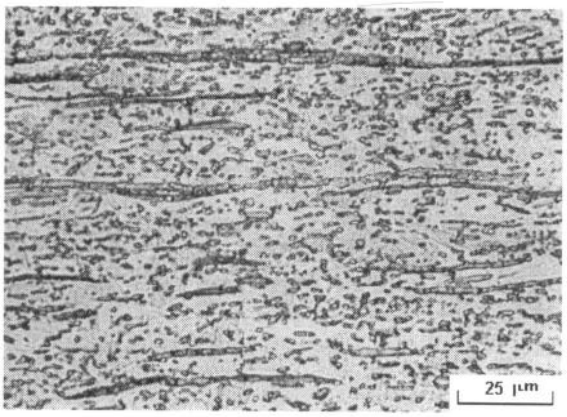

Figure 2 (b): Hot rolling at 870°C (HR1)

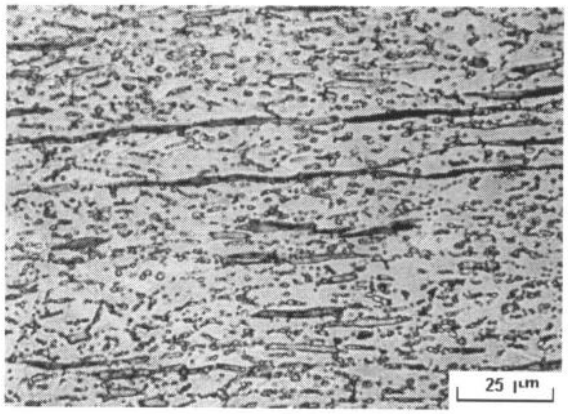

Figure 2 (c): Hot rolling at 1010°C (HR2)

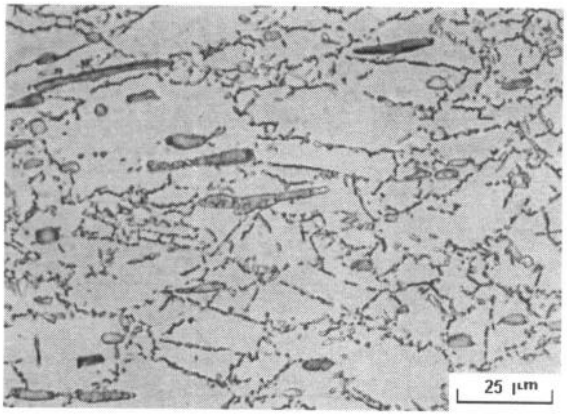

Figure 2 (d): Hot rolling at 1150°C (HR3)

Figure 2: Microstructure after TMP and direct aging

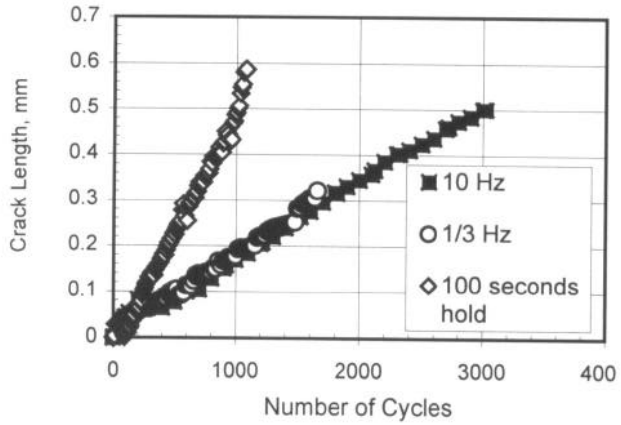

Figure 3 (a): Hot rolling at 870°C (HR1)

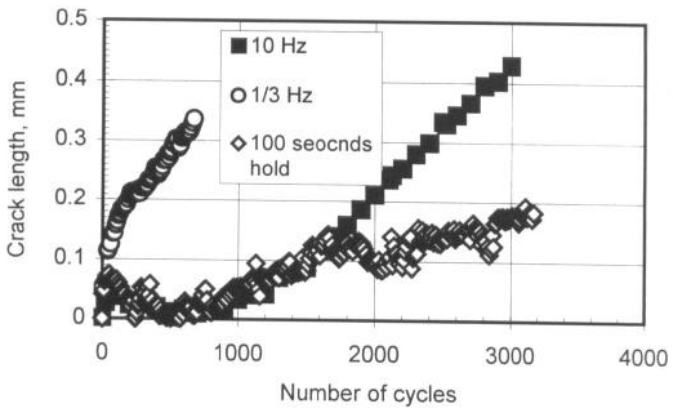

Figure 3 (b): Hot rolling at 1150°C (HR3)

Figure 3: Fatigue crack growth at ΔK=28 MPa$\sqrt{m}$ and 600°C

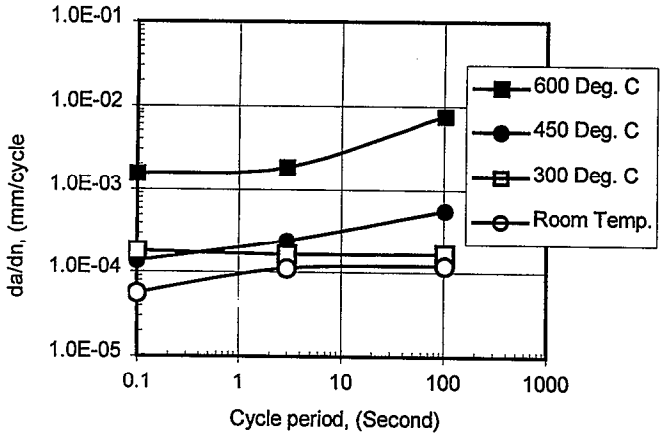

Figure 4 (a): Hot rolling at 1095°C(HR0)

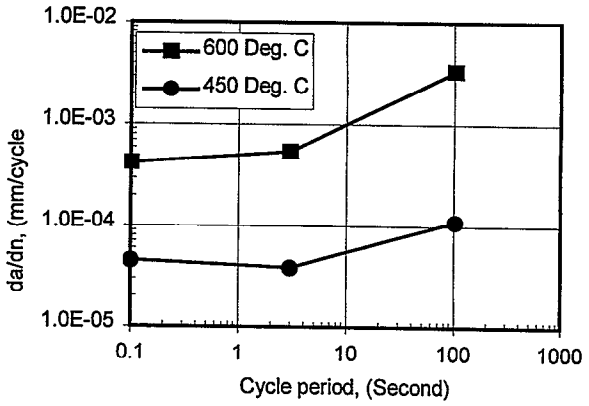

Figure 4 (b): Hot rolling at 870°C (HR1)

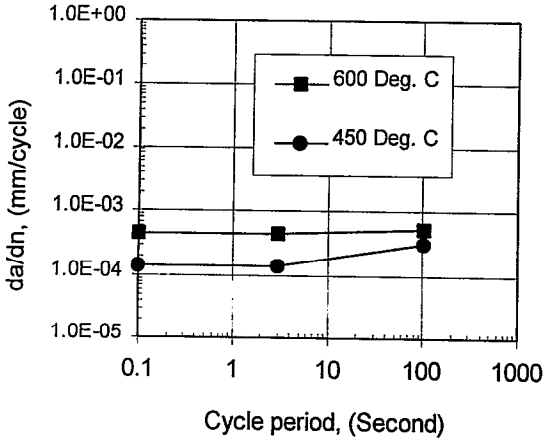

Figure 4 (c): Hot rolling at 1010°C (HR2)

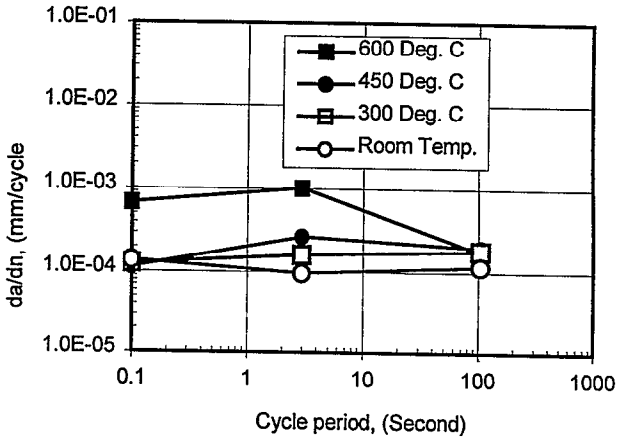

Figure 4 (d): Hot rolling at 11500°C (HR3)

Figure 4: Fatigue crack growth of TMP specimens at ΔK=28 MPa$\sqrt{m}$

Table III Fatigue crack growth (mm/cycle) at ΔK=28 MPa$\sqrt{m}$

Temperature (°C)	Frequency (Hz)	HR0	HR1	HR2	HR3
600	10	1.53×10^{-3}	4.17×10^{-4}	4.59×10^{-4}	6.72×10^{-4}
	1/3	1.84×10^{-3}	5.43×10^{-4}	4.50×10^{-4}	1.02×10^{-3}
	100 scconds Hold	7.51×10^{-3}	3.32×10^{-3}	5.45×10^{-4}	1.77×10^{-4}
450	10	1.36×10^{-4}	4.51×10^{-5}	1.43×10^{-4}	1.14×10^{-4}
	1/3	2.41×10^{-4}	3.80×10^{-5}	1.47×10^{-4}	2.67×10^{-4}
	100 seconds Hold	5.65×10^{-4}	1.11×10^{-4}	3.13×10^{-4}	2.01×10^{-4}
300	10	1.79×10^{-4}			
	1/3	1.65×10^{-4}			
	100 seconds Hold	1.67×10^{-4}			
Room Temp.	10	5.60×10^{-5}			
	1/3	1.12×10^{-4}			
	100 seconds Hold	1.21×10^{-4}			

(b). The slope of the linear portion of each curve represents the crack growth rate, which can be calculated by linear regression analysis. For the 870°C rolled material (HR1) as seen in Figure 3 (a), the crack growth rate for the 100 second hold test is 5 times higher than for the 10 Hz and 1/3 Hz tests, wherein the crack growth rate keeps constant. This is so called time-dependent fatigue crack growth and the phenomenon has been documented well in other alloys [10-12]. However, for the 1150°C rolled material (HR3), the crack growth rate for the 1/3 Hz test is dramatically higher than for the other two conditions as illustrated in Figure 3 (b). These observations will be discussed later.

Crack growth rates at different temperatures as a function of cycle period are shown in Figures 4 (a) to (d). Crack growth rates at 450°C and 600°C for material tested using the 100 second hold time rate is 5-10 times higher than for the 10 Hz and 1/3 Hz for the materials rolled at 1095°C (HR0) and 870°C (HR1). The difference in growth rate at those test temperatures is less pronounced with varying cycle times for the specimens rolled at 1010°C (HR2). However, for 1150°C rolled material (HR3), the crack growth rate at 600°C during the 100 second hold time test is significantly lower than in the case of the 10 Hz and 1/3 Hz tests. Further, the crack growth rate of 1150°C rolled specimen (HR3) during the 100 second hold test is also considerably lower than that for the specimens rolled at 1010°C, 1095°C, and 870°C. These findings demonstrate that an increase in the hot working temperature significantly decreases the time-dependent fatigue crack growth at 600°C for alloy 783. Crack growth rates at 300°C and room temperature for the specimens rolled at 1095°C and 1150°C were comparable for all three test conditions. This illustrates that at lower temperatures, crack growth is independent of rolling temperature, test frequency, and hold time. Fully understanding the relationship between microstructure and crack growth can provide the potential method to improve component life and enhance service temperature. Table III shows the data used in Figure 4.

Discussion

The effects of TMP on the microstructure and room tensile strength of alloy 783 as well as the TTT diagrams have been well documented [1-6]. In addition to the strengthening γ' precipitates developed during low temperature aging treatments, many precipitate phases may exist in the hot rolling temperature range. The equilibrium precipitation phase, β phase, has a solvus temperature around 1140°C. Since the β phase would not be coherent with the fcc matrix phase, they prefer to nucleate and grow along the defect sites in the alloy. Therefore, for HR1 and HR2, grain boundaries and dislocation networks are commonly decorated by the numerous β precipitates as seen in Figure 1 (b) and (c). As a result, the recrystallization will not easily take place during hot rolling because of retardation of β phases, and the structure consists of elongated, uncrystallized grains. However, when the hot rolling temperature is close to or above the β solvus, the recrystallization will occur during or after hot rolling. For HR3, dynamic recrystallization produced a very fine grain size with a serrated grain boundary structure. Some residual strains still remain due to the high deformation amount. In HR0, since the hot rolling reduction ratio is relatively low, there is a very fine equiaxed grain structure without deformation flow lines and with a serrated grain boundary structure.

Comparison of crack growth rates among four TMP microstructures are replotted in Figure 5, wherein transverse axis represents the temperature of TMP, with the origin point representing the HR0 processing. At a cycle-dependent stage, e.g. 10 and 1/3 Hz frequencies, four TMP specimens have a similar crack growth rate, which is simply determined by the pure mechanical driving force such as crack opening distance (COD) [13]. However, at hold time loading, the crack growth rate is drastically decreased with an increase of TMP temperature, i.e. the microstructure can have an extensive effects on FCP under the time-dependent condition.

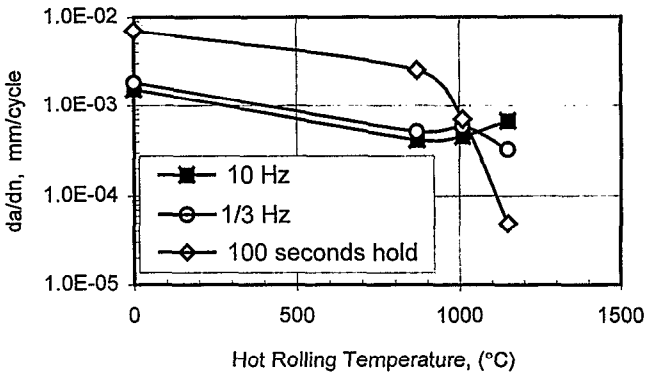

Figure 5: Fatigue growth rate against TMP Temperature at 600°C and ΔK=28 MPa√m

The fundamental mechanism causing the time-dependent crack propagation has been studied extensively. Conventionally three categories of theories, which are environmental effects, creep cracking effects, and strain rate effects respectively [13-17], have been proposed to explain the acceleration of crack growth under the time-dependent testing condition. Of course, complete separation of these three mechanisms may be impossible, while one of them generally becomes dominant in some alloys. Based on data generated in vacuum and other aggressive or inert gaseous environment for some superalloys, [11-13, 18-19] the environmental effect is believed to play the major role at elevated temperature crack growth. But the detailed mechanism of environmental effects is still not clear. In air, oxygen is the particular species responsible for the environmental effect. Presumably slow fatigue frequency allows oxygen atoms to be transported through the crack tip and to embrittle the grain boundaries ahead of the crack front. As a consequence, crack propagation is accelerated due to oxygen diffusion into grain boundaries ahead of the crack tip, and then time-dependent crack propagation occurs. It is important to note, however, that an environment, which can increase the crack growth rate under fatigue and creep loads, usually, does not produce significant general attack in unstressed materials. Thus, the stress assisted grain boundary oxidation (SAGBO) mechanism is considered to be responsible for time-dependent crack growth in this current study. It has been verified in alloy 718 that the SAGBO mechanism can cause the formation of a damage zone ahead of the crack tip during hold time of a sustained load. The damage zone, the size of which is a function of hold time, temperature, oxygen partial pressure, and stress intensity factor, can induce intergranular fracture and accelerate the crack growth rate [10-12, 20]. Therefore, based on the SAGBO mechanism and damage zone model, a phenomenological explanation for the observed crack

Therefore, based on the SAGBO mechanism and damage zone model, a phenomenological explanation for the observed crack growth behaviors in different TMP specimens of alloy 783 is proposed. When the fatigue frequency is high, e.g., 10 and 1/3 Hz, the crack growth rate is cycle-dependent and is determined by the cyclic stress intensity (ΔK), with only a limited effect of microstructure [13]. Lowering the frequency will enable oxygen diffusion to the grain boundaries producing a damage zone ahead of the crack tip. The damage zone causes intergranular fracture during crack growth and therefore accelerates the growth rate. This may explain the faster crack propagation rate observed with hold time for the 1095°C and 870°C hot worked specimens (HR0 and HR1) tested at 450°C and 600°C. Fractographs of these specimens show completely intergranular fracture as seen in Figure 6. It should be noted that the fracture surface of the HR1 specimen in Figure 6 (b) exhibits large amounts of precipitates along the grain boundary areas and fluctuated fracture paths. These precipitates are believed to be β phases, which may retard the crack propagation during intergranular fracture and decrease the effects of oxidation on the grain boundary and matrix [1-2, 21]. Also, the residual strain structure referred to as stringers, which are dislocation networks and segregation of β phase, can provide the preferential sites for oxygen diffusion during the build-up of the damage zone. The combination of the above effects is expected to enhance the time-dependent fatigue crack growth resistance. Thus, the crack growth rate of the HR1 specimen would be lower relative to the HR0 specimen during time-dependent fracture.

It is interesting to note that specimens rolled at 1010°C had many secondary parallel cracks as seen in Figure 7 (a). These secondary cracks were in the primary crack propagation direction with the interspacing about 100μm, which is almost equal to the distance between parallel β phase stringers as shown in Figure 1(c). These β phase stringers presumably provide preferential oxygen absorption sites resulting in embrittlement and secondary cracking along the stringers. In this type of cracking, stress concentration at the crack tip can be released to form multiple parallel cracks, which will not show a time-dependent behavior under cyclic-loading [22]. High magnification fractograph of the secondary crack areas show that the fracture mode is predominantly transgranular, and the fracture surface is covered by many particles (mostly β phase) and is relatively rough as shown in Figure 7(b).

Secondary cracks were also found in the specimen hot rolled at 1150°C (HR3) as shown in Figure 8. Interspacing of these cracks was approximately 5-10μm. The fracture surface demonstrates an obvious border between tests of hold time at 600°C and high frequency (10 Hz) at 450°C. There exist many secondary cracks in hold time specimen tested at 600°C. High magnification micrographs of these areas exhibits an intergranular fracture path and a ductile appearance with many dimples as seen in Figure 8 (b). However, in the high frequency specimen tested at 450°C, the fracture mode is typically of a microvoid nature. The ductile fracture feature in material hot rolled at 1150°C (HR3) in hold time condition could be ascribed to the serrated boundaries in this material induced by TMP as shown in Figure 2(d). Serrated grain boundaries are thought to restrict grain boundary sliding which increases the fracture path resulting in better crack growth behavior [23-24]. This could explain the better crack growth resistance of the 1150°C hot worked material tested at high temperature under hold time mode.

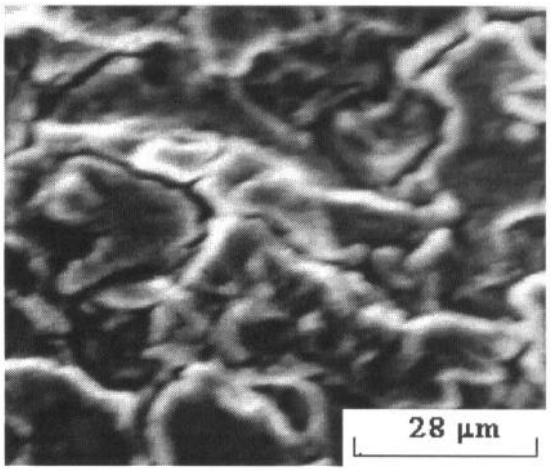

Figure 6 (a): Hot rolling at 1095°C (HR0)

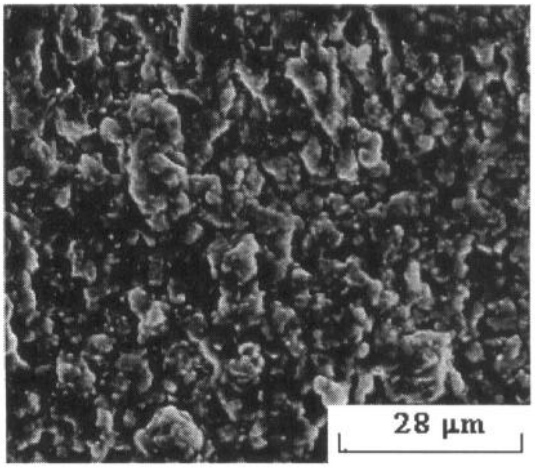

Figure 6 (b): Hot rolling at 870°C (HR1)

Figure 6: Fractograph of SEM at ΔK=28 MPa√m, 600°C, and 100 seconds hold

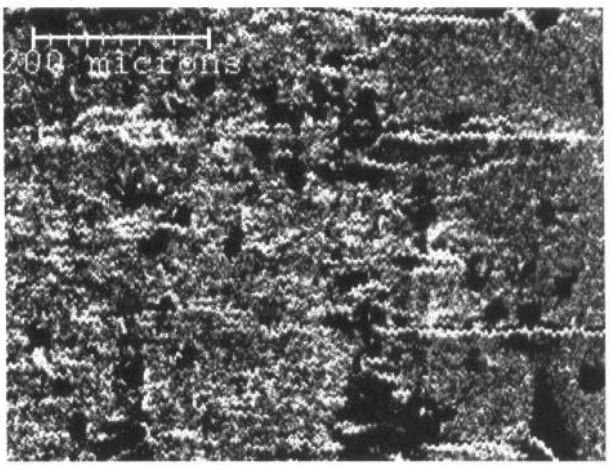

Figure 7 (a): Secondary crack in HR2

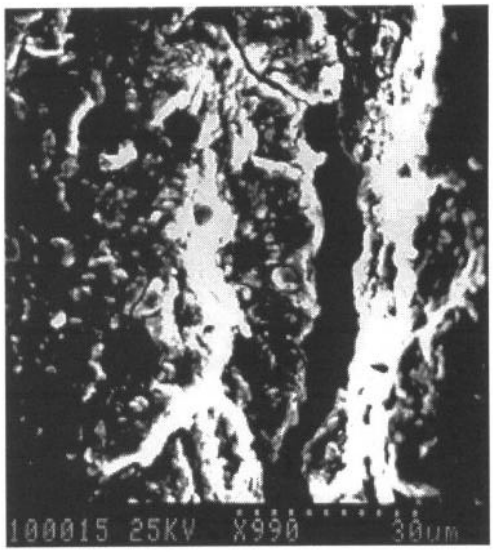

Figure 7 (b): High magnification of (a)

Figure 7: Fractograph of SEM for hot rolling at 1010°C at ΔK=28 MPa$\sqrt{m}$, 600°C, and 100 seconds hold

Conclusions

Four different microstructures of INCONEL Alloy 783 have been identified as the result of different TMP parameters and their fatigue crack propagation behaviors have been evaluated under time-dependent testing conditions. The data suggests the following:

1. Microstructures induced by the thermomechanical processing (TMP) have substantial effects on time-dependent fatigue crack propagation behavior in alloy 783, but little influence on cycle-dependent crack growth rate.

2. A deformed grain structure without recrystallization and with a large number of β phase particles distributed within the grain increases the resistance to crack propagation under time-dependent condition. The appearance of secondary cracks weakens the effects of the time-dependent behavior on the crack growth rate, together with a change of fracture mode.

3. The introduction of grain boundary serration produced by TMP can significantly improve the resistance to fatigue crack propagation under time-dependent condition.

4. SAGBO and an environmentally induced damage zone at the crack tip are believed to play a major role in time-dependent fatigue propagation in alloy 783 at elevated temperatures.

Acknowledgments

The authors would like to thank Specials Metal Corporation at Huntington, WV for supplying the INCONEL alloy 783 used in this study and contributing insight on this project. Many thanks are also due to F. J. Veltry and J. M. Davis at Specials Metal Corporation for their technical support in metallographic sample preparing. This study was sponsored by West Virginia EPSCOR program.

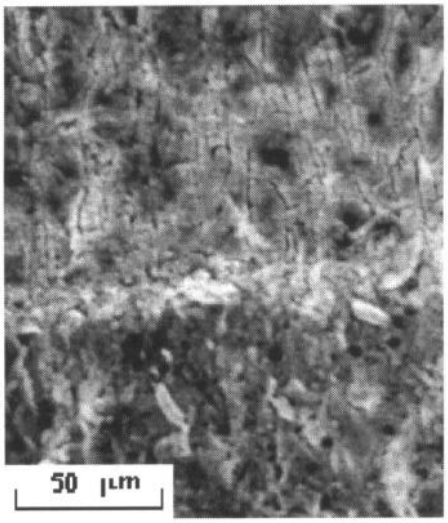

Figure 8 (a): Fracture surface in HR3

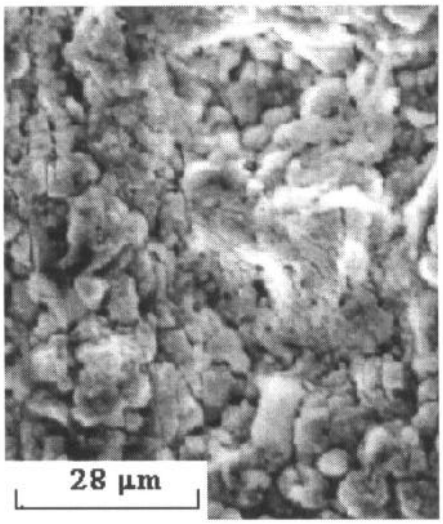

Figure 8 (b): High magnification of (a)

Figure 8: Fractograph of SEM for Hot rolling at 1150°C under ΔK=28 MPa$\sqrt{m}$ and 600°C

Reference

1. J. S. Smith and K. A. Heck, "Development of Low Thermal Expansion, Crack Growth Resistant Superalloy" Superalloys 1996, edited by R. D. Kissinger, D. J. Deye, D. L. Anton, A. D. Cetel, M. V. Nathal, T. M. Pollock, and D. A.Woodford, The Minerals, Metal & Materials Society, Seven Spring, PA, USA, 1996, 91-100.

2. K. A. Heck, J. S. Smith, R. Smith, "Inconel alloy 783: An oxidation Resistant, Low Expansion Superalloy for Gas Turbine Applications," International Gas Turbine and Aeroengine Congress & Exhibition, Birmingham, UK, June 10-13, 1996: 1-8.

3. K. A. Heck, D. F. Smith, M. A. Holderby and J. S. Smith, "Three-phase Controlled Expansion Superalloys with Oxidation Resistance" Superalloy 1992, edited by S. D. Antolovich, R. W. Stusurd, R. A. MacKay, D. L. Anton, T. Khan, R. D. Kissinger, D. L. Klarstrom, The Minerals, Metal & Materials Society, Seven Spring, PA, USA, 217-226.

4. M. M. Morra, " Stress Accelerated Grain Boundary Oxidation of INCOLOY Alloy 908 in High Temperature Oxygenous Atmosphere" (Ph.D. thesis, Massachusetts Institute of Technology, 1995), 16-17.

5. S. Mannan and J. deBarbadillo, "Long Term Thermal Stability of INCONEL Alloy 783," International Gas Turbine and Aeroengine Congress & Exhibition, Stockholm, Sweden, June 2-5, 1998, 1-10.

6. B. E. Higginbotham, K. M. Chang, S. Mannan, J. J. deBarbadillo, "Microstructure and Property Control of INCONEL 783 Through Thermomechanical Processing (TMP)," Proceedings of the 1st International Non-Ferrous Processing and Technology Conference, St. Louis, Missouri, 10-12 March 1997, 483-489.

7. P. Shahinian and K. Sadananda, "Effects of Stress Ratio and hold-Time on Fatigue Crack Growth in Alloy 718," The American Society of Mechanical Engineers (Proc.), June 25-29, 1979, 1-9.

8. K. Sadananda and P. Shahinian, "Effect of Microstructure on Creep-fatigue Crack Growth in Alloy 718, Res. Mechanica. Vol. 1, 1980, 109-128.

9. H. Ghonem and D. Zheng, "Frequency Interactions in High-Temperature Fatigue Crack Growth in Superalloys," Metall. Trans. A, Vol. 23 A, Nov. 1992, 3067-3072.

10. K. M. Chang, M. F. Henry and M. G. Benz, "Metallurgical Control of Fatigue Crack Propagation in Superalloys," JOM, Vol. 42, No.12, Dec. 1990, 29-35.

11. K. M. Chang, "Elevated Temperature Fatigue Crack Propagation After Sustained Loading," Effects of Load Thermal Histories on Mechanical Behavior of Materials (Proc.), TMS Spring Meeting, Denver, CO, 1987, ed., P. K. Liaw et al., AIME-TMS, 13-26.

12. K. M. Chang, "A Phenomenological Theory for Time-Dependent Fatigue Crack Propagation in High-Strength Superalloys," (G.E R & D Report, No: 91CRD066, March 1991, 1-19.).

13. D. L. Davidson and J. Lankford, "Fatigue Crack Growth in Metals and Alloys: Mechanisms and Micromechanics," International Mater. Rev. Vol. 37, No: 2, 1992, 45-75.

14. K. Sadananda and P. Shahinian "High Temperature Time Dependent Crack Growth, Micro and Macro mechanics of Crack Growth," Proceeding of Symposium, Metallurgical Society of AIME, Warrendale, Pa, 1982, 119-130.

15. D. A. Woodford and R .H. Bricknell, "Environmental Embrittle of High Temperature Alloys by Oxygen," Treatise on Materials Science and Technology, Vol.25, 1983, 157-196.

16. S. Floreen and R. H. Kane, "A Critical Model for the Creep Fracture of Nickel-Base Superalloys," Metall. Trans. A, Vol.7 A, Aug. 1976, 1157-1160.

17. J. Z. Xie, Z. M. Shen, and J. Y. Hou, "Fatigue Crack growth Behaviors in Alloy 718 at High Temperature," Superalloy 718 625 and Various Derivatives, edited by E. A. Loria, The Minerals, Metal & Materials Society, 1997, 687-594.

18. S. Floreen and R. H. Kane, "Effects of Environment on High-Temperature Fatigue Crack Growth in a Superalloy," Metall. Trans. A, Vol. 10 A, Nov. 1979, 1745-1751.

19. K. Sadananda and P. Shahinian, "Effect of Environment on Creep Crack Growth Behavior in Austenitic Stainless Steels under Creep and Fatigue Conditions," Metall. Trans. A, Vol. 11A, Feb. 1980, 267-276.

20. W. Carpenter, B.S.-J. Kang and K. M. Chang, "SAGBO Mechanism temperature Cracking Behavior of Ni-base Superalloys," Superalloy 718 625 and Various Derivatives, edited by E. A. Loria, The Minerals, Metal & Materials Society, 1997, 679-688.

21. J. S. Lyons, A. P. Reyonlds and J. D. Clawson, "Effect of Aluminide Particle Distribut-ion on the High Temperature Crack Growth Characteristics of A Co-Ni-Fe Superalloy," Scripta Mater., Vol.37, No:7, 1997, 1059-1064.

22. K. M. Chang, "Improving Crack Growth Resistance of IN 718 Alloy Through Thermomechanical Processing," (G.E. Report, No. 85CRN187, Oct. 1985, 1-12).

23. R.Raj and M.F.Ashby: On Grain boundary sliding and diffusion creep, Metall. Trans. A, Vol. 2, April 1971: pp. 1113-1127.

24. J. M. Larson and S. Floreen, "Metallurgical Factors Affecting the Crack Growth Resistance of a Superalloy," Metall. Trans. A, Vol. 8 A, Jan. 1977, 51-55.